Transactions of the Materials Research Society of Japan 29 [2] 581-586 (2004)

Observation of ion implanted materials using 3D electron microscope

Tomohiro Kobayashi and Masaya Iwaki
The Institute of Physical and Chemical Research (RIKEN),
Advanced Development and Supporting Center
2-1 Hirosawa, Wako, Saitama 352-0198, Japan.
Fax: 81-48-462-4623, e-mail: t-koba@riken.go.jp

Three-dimensional (3D) observation of nanostructures is useful for a new material design especially for ion-implanted materials containing nanoparticles. In this study, metallic nanoparticles formed in sapphire and polyimide substrates by high-dose ion implantation have been observed using a new scanning transmission electron microscope (STEM) that has been developed for the 3D observation. The implanted specimens were processed as 100-300 nm diameter cylinders, which included the implanted layer, produced using a focused ion beam (FIB). STEM observations were performed by rotating the specimens around the axis of the cylinder. Ni atoms implanted in sapphire formed particles aligned with the surface plane without requiring an annealing stage. The Cu particles in sapphire were disc-shaped and arranged parallel to the surface, located in a highly damaged layer due to the anisotropy in diffusion. The Cu particles formed in polyimide were uniformly dispersed at depths between 10 and 70 nm from the surface. The observations showed migration of Cu atoms towards the surface, and the lattice images of Cu nanoparticles indicated that each particle consisted of a single crystal. Tungsten-carbide nanoparticles were found in high-resolution TEM (HRTEM) observation in W implanted polyimide. The depth-resolved profile of electron mean free path was analyzed with electron energy loss spectroscopy (EELS). The observations suggest that alteration reached about four times further than the mean ion range.

Key words: nanoparticle, ion implantation, sapphire, polyimide, 3D-EM

1. INTRODUCTION

Metallic nanoparticles formed in insulating materials have great potential for application in novel devices because of their peculiar characteristics, such as their optical nonlinearity [1] and magnetic properties [2]. Ion implantation is one of the most useful methods to fabricate nanoparticles in the surface layer of materials [3]. We have previously studied the structures of such particles and the electrical properties of implanted layers [4,5]. Characterization and control of the distribution, the shape, the growth direction, and the crystal structure of the particles are important in designing new devices.

Recently, a new electron microscope, the 3D-EM, has been developed for the three-dimensional (3D) observation of nanostructures [6]. It was constructed by a joint research team composed of members from RIKEN, the Japan Atomic Energy Research Institute (JAERI), Nagoya University, Kogakuin University, Hitachi Ltd., and Hitachi High-Technologies Corporation. The project was supported by the Intellectual Foundation System of the Special Coordination Funds for promoting Science and technology of the Japanese government. The instrument is based on a Hitachi HF-3000 300 kV FE-TEM/STEM and is equipped with an accurate eucentric sample stage, an automatic focusing system, and a sample-position correction system. The system was designed to obtain images easily and quickly by rotating a sample over a wide-angle range.

The automatic focusing system (feedback to the Scherzer focus) uses a new algorithm based on the transfer function of STEM imaging and it can also adjust astigmatism. The method is designed to work independent of specimen object function and is accomplished in a practical time. The image drift is accurately measured and specimen stage is controlled depending on the measured values. The system was made with digital signal processor (DSP) hardware modules and the control is real-time.

The 3D-EM can also carry out electron energy loss

spectroscopy (EELS) with high energy resolution. Our final goal of the 3D-EM development is to analyze composition and bonding states in nanometer sized area using this instrument in combination with optimized electron irradiation and detection conditions.

Figure 1 shows the developed points of the 3D-EM in the project. The system has been shown to be useful for the characterization of defects in semiconductor devices. In this study, we have observed the shape and the distribution of metallic nanoparticles formed in insulators using the 3D-EM.

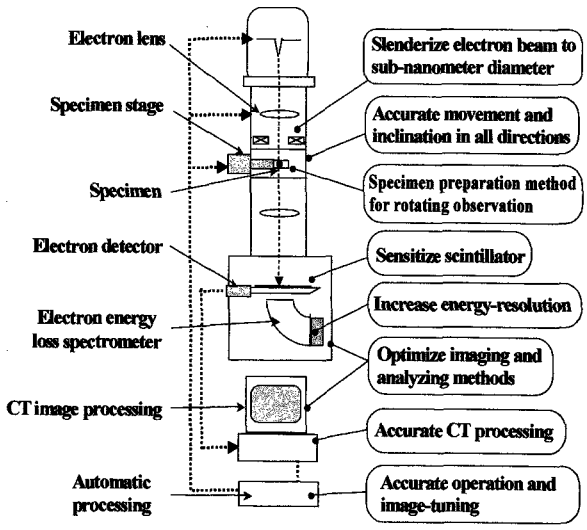

Fig.1 Developing elements of the 3D-EM project.

2. EXPERIMENTAL

2.1 Nanoparticle formation

The (110) and (001) surfaces of single crystal α-Al_2O_3 (sapphire) specimens were implanted with 3 MeV Ni ions at a fluence of 1.6 x 10^{18} cm^{-2} using a tandem accelerator in Tokyo University, and 380 keV Cu ions at a fluence of 2.7 x 10^{17} cm^{-2} using an electrostatic accelerator in JAERI. The maximum concentration of implanted elements was greater than 20%. During implantation, the specimens were tilted 5° from the perpendicular axis. The current density used was 1-2 μA/cm^2, the pressure was 1 x 10^{-5} Pa, and the temperature on the rear surface of the specimens was around 380 K for Ni implantation, and 350 K for Cu implantation. The mean ion ranges, calculated by TRIM code [7], were 1.2 μm for Ni, and 160 nm for Cu. Thermal annealing was carried out on Cu implanted specimens at 1073 K for 1 h in vacuum (pressure of 7 x 10^{-4} torr).

A polyimide film produced by Toray-DuPont (Kapton, 30 μm thick) was implanted with 100 keV Cu, 190 keV W and 40 keV N ions of the relevant dosages. The mean ion ranges for these implantations were set at about 150 nm, as calculated by TRIM code. The fluence was 5×10^{16} cm^{-2} for Cu and N implantation and 1×10^{17} cm^{-2} for W implantation, and the current density was kept to 0.1-3.0 μA cm^{-2} at a pressure below 1×10^{-4} Pa. During irradiation, the temperature on the rear side of the specimens was below the glass transition temperature of polyimide (360 °C). The nitrogen implantation was performed to make a damaged specimen without metal ions for reference.

2.2 Sample processing

The surface layer of the implanted specimens was cut using an FIB system (Hitachi FB-2000A) and a wedge-shaped piece was took out using a micro-sampling system employing a tungsten needle manipulator. Then, the piece was transferred to the top of a pin-shaped sample holder, and fixed using a beam-assisted tungsten deposition system. The surface of the sample piece was removed, leaving a cylinder 100 – 300 nm in diameter for the rotating STEM observations, as shown in Fig.2. The rotating axis was parallel to the main cylinder axis. We could observe the specimen without any of the obstacles and change in thickness that is a problem when rotating planar samples in conventional cross-section observations.

The polyimide specimens for EELS observation were also processed using FIB. The cross-sectional specimens were planed down on both sides to leave a 100-nm-thick part for line-analysis.

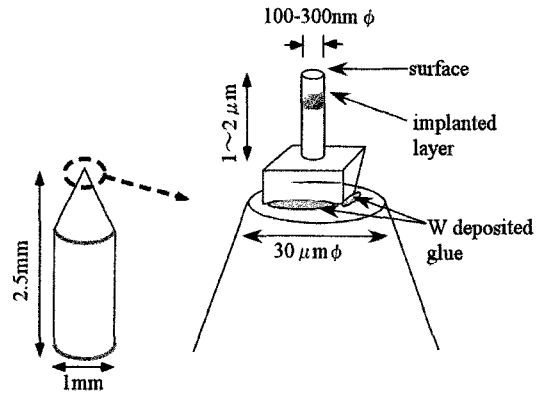

Fig.2 The pin-shaped sample holder and cylindrical sample prepared using an FIB and a micro-sampling system.

2.3 TEM observations

The cylindrical specimens were observed under bright-field (BF) and high-angle annular-dark-field (HAADF) STEM mode at 300 keV. The sample rotating range was 180°, and images were taken in 3° steps. The observations were performed using an electron current of 30μA under a pressure below 3 x 10^{-6} Pa. The reconstruction of the 3D images by tomography or topography was not developed in this study, because of the non-linearity in the electron intensity from

crystalline samples obtained by BF-STEM mode giving precedence to contrasts in images.

3. RESULTS AND DISCUSSION

3.1 Nanoparticles in sapphire

Figure 3 shows a SEM image of the 3 MeV Ni implanted specimen. In this case, two cylinders are fabricated. The detailed BF-STEM image of the implanted layer is shown in Fig.4. The mean depth of implanted layer is 1.3 μm from the surface, which agrees well with the calculated value. The implanted Ni atoms form nanoparticles around 5 to 10 nm in diameter aligned along the (110) plane. This result agrees with the electrical resistivity measurements, which indicate that the implanted Ni atoms form particles without any post-implantation thermal annealing [4]. A rotating observation showed that the particles were widely distributed in a plane, rather than aligned in a string-like manner. Although the mechanism of the formation and the arrangement of the particles is still not clear, we presume that excess impurities will tend to collect in fissures along the (110) plane formed by internal stress.

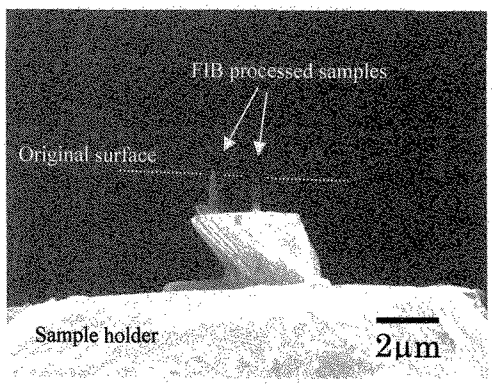

Fig.3 A cylindrical samples fabricated from 3 MeV Ni implanted sapphire (SEM image).

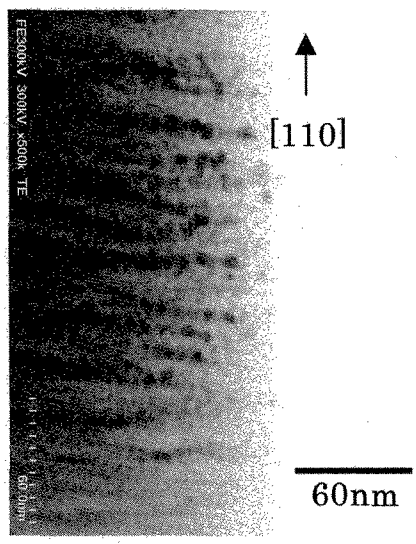

Fig.4 Ni nanoparticles formed in sapphire (BF-STEM image).

In the 380 keV Cu implanted specimens, no particles were observed without carrying out post-implantation annealing. Figure 5 shows BF-STEM images taken by rotating a cylinder of a sample that was Cu-implanted and then annealed. The implantation was performed perpendicular to the (001) plane. Large precipitates were observed at a depth from 130 to 150 nm, which were composed of irregular plate-shaped particles, with some precipitates being connected to each other. These observations indicate that the diffusion speed in the (001) plane direction at a depth that is a little shallower than mean ion range is much faster than that in the perpendicular direction due to the high level of damage induced by the displacement collisions. The moire patterns shown in Fig.6 indicate that particles were composed of single crystals.

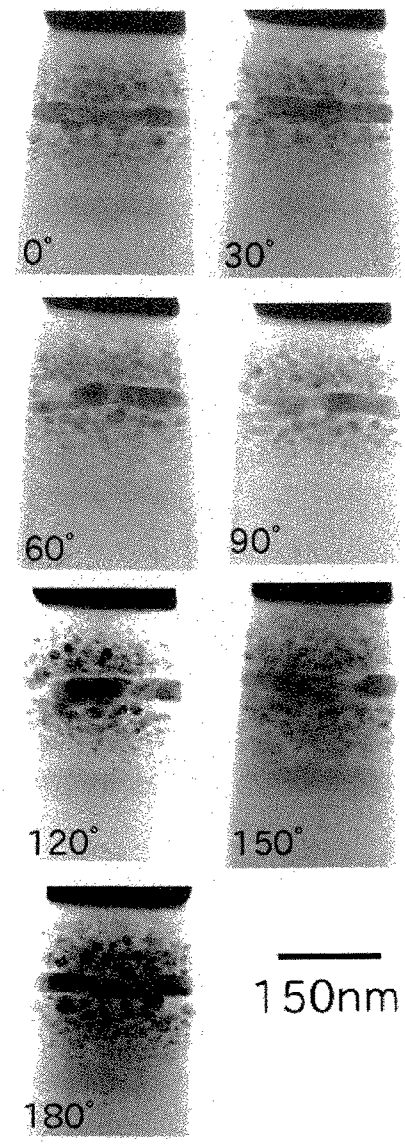

Fig.5 A rotation series of a cylinder sample implanted with 380 keV Cu at a fluence of 2.7 x 10^{17} cm^{-2} followed by thermal annealing (BF-STEM image).

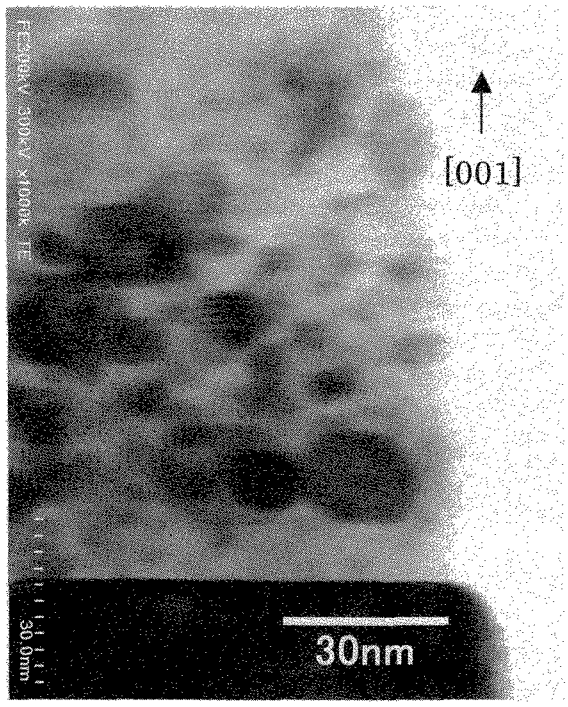

Fig.6 Moire patterns of Cu nanoparticles formed at depths from 30 to 120 nm from the surface.

3.2 Nanoparticles in polyimide

3.2.1 TEM observations

Figure 7 shows BF-STEM images of the 100 keV Cu implanted polyimide specimen. The Cu particles had diameters between 10 and 20 nm, and were uniformly dispersed at depths of 10 to 70 nm. The rotating observation results show that the particles do not make contact with each other. The contrast of each particle changed dramatically under rotation, and this implies that the particles have a crystalline structure.

The region from the surface to a depth of around 100 nm is stable against the electron beam because carbonization was already well progressed due to the implantation procedure. On the other hand, the deeper region was degraded by the electron beam, and a decrease in density was observed. The discharged gas will be a source of contamination accumulating on the surface of the cylinder, and this was not seen in the sapphire specimens.

Figure 8 shows an HAADF-STEM image of Cu nanoparticles. The fine structure of each particle was observed as a result of the change in the contrast caused by the difference of a direction of crystals. The results reveal that the mobility of Cu atoms in polyimide under irradiation is quite high.

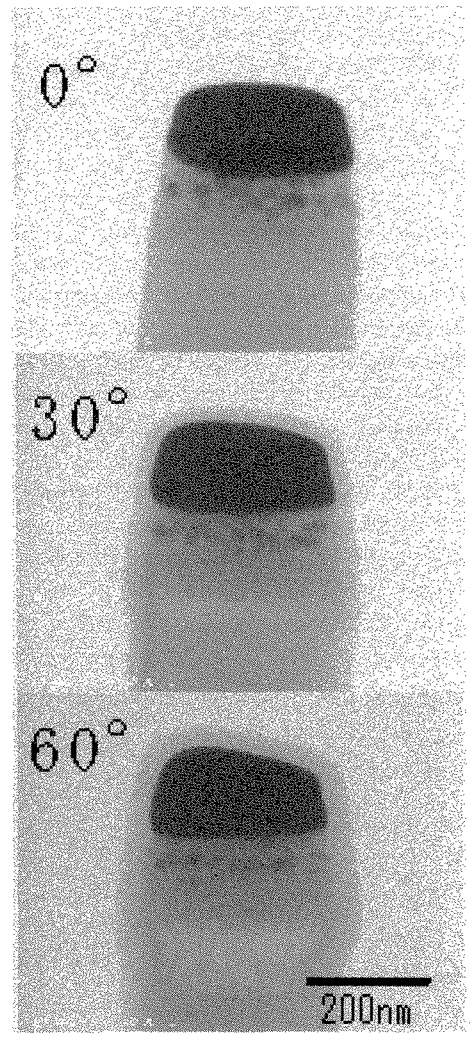

Fig.7 A rotation series of a cylinder sample implanted with 100 keV Cu at a fluence of 5 x 10^{16} cm^{-2} without any thermal annealing (BF-STEM image).

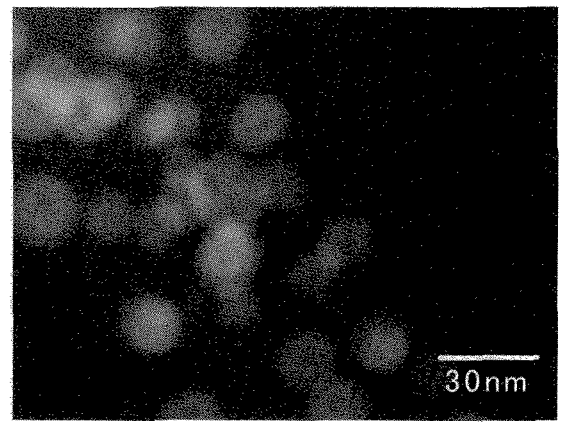

Fig.8 An HAADF-STEM image of Cu nanoparticles formed in a carbonized layer of polyimide.

Fig. 9 shows a HRTEM image of nanoparticles. Each particle was almost perfectly spherical and consisted of crystalline copper.

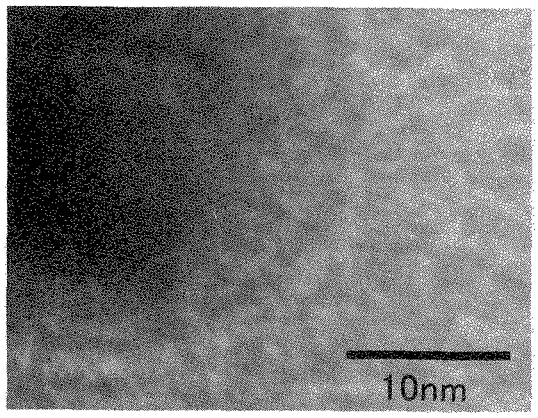

Fig.9 A HRTEM image of a copper nanoparticle.

Fig. 10 shows a cross-sectional TEM image of the W implanted surface. The central depth of implanted tungsten is about 150 nm. This means that implanted tungsten did not migrate macroscopically.

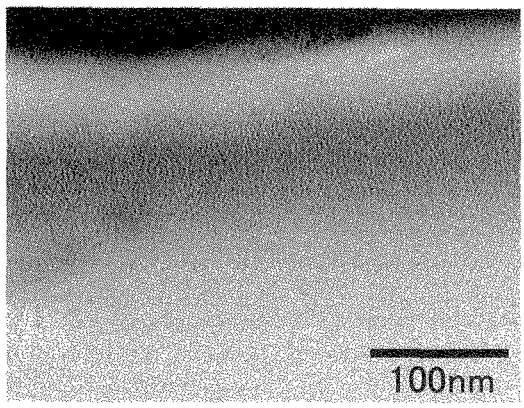

Fig.10 A cross-sectional TEM image of tungsten implanted polyimide surface.

Fig. 11 shows a HRTEM image around the depth of the mean ion range. The image shows the presence of particles of about 2 nm diameter that were not observed in our previous study due to thermal deformation of microtomed samples during TEM observation [5]. Crystalline particles were not observed in the image and a diffraction pattern showed no distinct ring. These particles would have been tungsten with carbon and a small amount of oxygen, judging from our previous results of X-ray photoelectron spectroscopy (XPS) [8]. In this case, diffusion of implanted tungsten atoms was localized, in contrast to the case for copper.

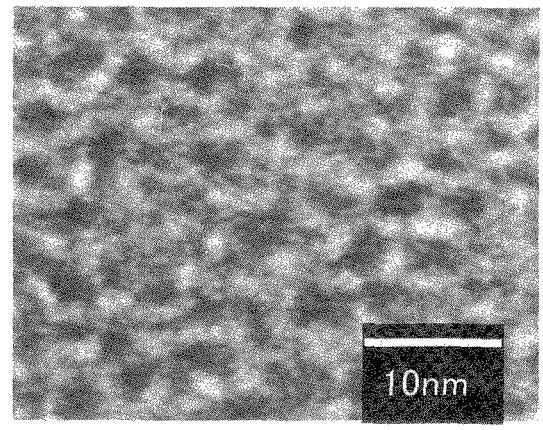

Fig. 11 A HRTEM image of tungsten implanted polyimide at a depth near the mean ion range.

3.2.2. Electron mean free path of implanted layers

In this study, we observed the depth profiles of mean free path for inelastic scattering using EELS. Total mean free path for inelastic scattering, λ, is given by

$$t/\lambda = \ln(I_t/I_0),$$

where t is the sample thickness, I_0 is the area of the zero-loss peak, and I_t is the total area of whole spectrum [9]. The thickness of FIB-processed specimens increases at a constant rate in the direction perpendicular to the surface plane because of the spread of the processing beam. We calibrated this increase in thickness by using an un-implanted specimen. Fig. 12 shows the depth profile of the normalized mean free path of the Cu implanted specimen (a), the W implanted specimen (b), and the N implanted specimen (c), with the distribution of ions being calculated by TRIM code. The normalization is carried out using the mean value of λ between the depths of 600 and 800 nm for Cu and W implanted specimens and 400 and 600 nm for the N implanted specimens, which is described as λ_0. The decrease in λ/λ_0 was observed at a depth of around 400 nm for the Cu and W implanted specimens. This means that alteration in the polyimide film reaches about four times further than the mean ion range. The reasons for the alteration is still not clear; one reason may be a compaction in volume because of the heating effect during implantation. The λ/λ_0 values are greater than 1 at the surface of the N implanted and Cu implanted specimens, indicating that the density at the surface was decreased by gas elimination. On the other hand, in the W implanted specimen, the low-density surface did not remain, because of the sputtering during implantation. In the Cu implanted specimen, λ/λ_0 is minimized at a level

shallower than the mean ion range. This result supports the TEM observation that the Cu atoms migrate toward the surface.

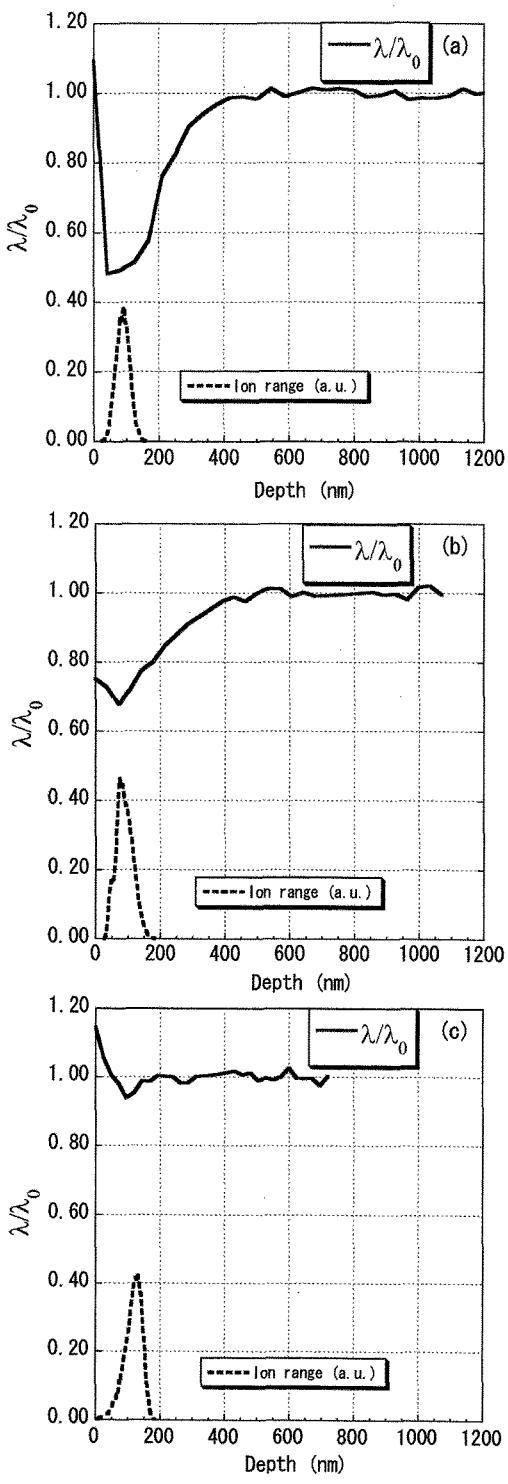

Fig. 12 Depth profiles of normalized electron mean free path and calculated mean ion range of (a) Cu implanted, (b) W implanted, and (c) N implanted specimens.

4. SUMMARY

The distribution and the shape of metallic nanoparticles formed in sapphire and polyimide by ion implantation were observed using 3D-EM. The peculiar distribution of Ni particles and complicated shape of Cu particles in sapphire were elucidated by the rotating observation. Observation with higher magnification focused on a single particle will make the shape of Cu particles in polyimide clearer. W nanoparticles were discovered; they contained carbon and were not crystalline. The alteration during implantation reached about four times further than the mean ion range in metallic ion implantation. The time required for adjusting position and focus was extremely reduced by the newly developed systems. Rotating observation was impossible without the system due to the degradation and the deposition of contamination by electron irradiation especially in the polyimide specimen.

REFERENCES

[1] Y. Takeda, C. G. Lee and N. Kishimoro, *Nuclear Instruments and Methods in Physics Research B.*, **190**, 797-801 (2002).

[2] E. Alves, C. McHargue, R. C. Silva, C. Jesus, O. Conde, M. F. da Silva and J. C. Soares, *Surface Coatings Technology*, **128-129**, 434-439 (2000).

[3] A. Meldrum, L. A. Boatner and C. W. White, *Nuclear Instruments and Methods in Physics Research B.*, **178**, 7-16 (2001).

[4] T. Kobayashi and T. Terai, *Nuclear Instruments and Methods in Physics Research B*, **116**, 187-190(1996).

[5] T. Kobayashi, T. Iwata, Y. Doi and M. Iwaki, *Nuclear Instruments and Methods in Physics Research B*, **175-177**, 548-553(2001).

[6] M. Koguchi, H. Kakibayashi, R. Tsuneta, M. Yamaoka, T. Niino, N. Tanaka, K. Kase and M. Iwaki, *Journal of Electron Microscopy*, **50(3)**, 235-241(2001).

[7] J. F. Ziegler, J. P. Biersack and U. Littmark, "The Stopping Range of Ions in Solids", Pergamon Press, New York, 1985.

[8] T.Kobayashi, A.Nakao and M.Iwaki, *Surface and coatings technology*, **158-159**,399 (2002).

[9] R. F. Egerton, "Electron Energy-Loss Spectroscopy in the Electron Microscope", Plenum, New York, 1996, p.302.

(Received October 9, 2003; Accepted January 20, 2004)